

# Vertical Gradients of Refractivity in the Mesosphere and Atmosphere Retrieved from GPS/MET and CHAMP Radio Occultation Data

Alexander Pavelyev<sup>1</sup>, Jens Wickert<sup>2</sup>, Yuei-An Liou<sup>3</sup>, Kiyoshi Igarashi<sup>4</sup>, Klemens Hocke<sup>4</sup>, Cheng-Yung Huang<sup>3</sup>

<sup>1</sup> IRE RAS, Fryazino, Vvedenskogo sq. 1, 141191 Moscow region, Russia  
*agp117@ire216.msk.su*

<sup>2</sup>GFZ-Potsdam, Telegrafenberg, 14473 Potsdam Germany, *wickert@gfz-potsdam.de*

<sup>3</sup>CSRSR, National Central University, Chung-Li, 320, Taiwan. *yueian@csrsr.ncu.tw*

<sup>4</sup>Communication Research Laboratory, Independent Administrative Institution 4-2-1, Nukui-Kita Machi, Koganei-shi, Tokyo 184-8795 Japan, *igarashi@crl.go.jp*

**Summary.** Fine structures in the vertical gradient of the electron density have been retrieved by means of analysis of the amplitude of radio occultation (RO) data in sporadic E-layers (heights interval 85-110 km). Maximum values of the positive gradients  $45 \cdot 10^9$ ,  $48 \cdot 10^9$ ,  $25 \cdot 10^9$ ,  $29 \cdot 10^9$  [ $\text{m}^{-3}\text{km}^{-1}$ ] are located at levels 92, 105 km (GPS/MET event 0393) and 93.5, 100 km (GPS/MET event 0583). Variations in the vertical gradient of refractivity in the atmosphere have been found for CHAMP RO event 09. Vertical gradient of refractivity changes in interval  $\pm 5$  N-units/km (height interval 3-10 km) and  $\pm 0.5$  N-units/km between levels 11 and 18 km. Vertical distribution of temperature gradient between level 3-37 km reveals features at height 4-6, 9-10 km with positive values of about 6-9 °K/km. Amplitude RO data analysis may be used for detailed retrieving vertical gradients of refractivity and temperature in the atmosphere and electron density in the lower ionosphere during CHAMP and future COSMIC RO missions.

**Key words:** radio holography, occultation, atmosphere, mesosphere, ionosphere, refractivity, temperature

## 1 Introduction

RO GPS/MET experiments revealed a new problem: high precision of radio navigational fields requires more accurate and effective scientific methodology for inferring atmospheric, mesospheric and ionospheric parameters. For solution of this problem radio holographic technology may be used. Early *Marouf and Tyler, 1982, Lindal et al., 1987*, applied radio holography approach to analysis of Voyager 1 RO data. The backward method was suggested for RO investigation of the Earth's atmosphere [*Gorbunov and Gurvich, 1996; Karayel and Hinson 1997*] with the aim of heightening vertical resolution. Back propagation and radio holographic methods have been proposed to study ionospheric irregularities by *Gorbunov et al., 2002, Sokolovskiy et al., 2002, Pavelyev et al., 2002. Pavelyev 1998, Hocke et al., 1999, Igarashi et al., 2000*, developed method of radio holographic

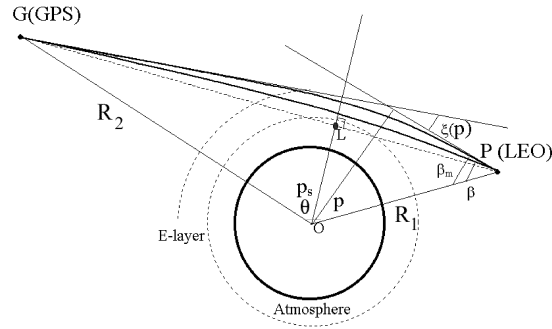


**Fig. 1.** Scheme of GPS/MET and CHAMP radio occultation experiments.

analysis of RO data. *Igarashi et al., 2000*, showed that radio holography approach consists in application of focused synthetic aperture method for combined analysis of phase and amplitude variations in RO signal. *Igarashi et al., 2001*, demonstrated high vertical resolution of the radio holographic method (of about 20-70 m) by means of retrieving weak signals reflected from the sea surface in GPS/MET RO data. *Igarashi et al., 2000, 2001, 2002*, presented first results of measuring vertical gradients of the electron density in the lower ionosphere. Aim of this paper is to demonstrate possibility of detailed measurements of gradients of the electron density in the mesosphere and refractivity in the atmosphere from amplitude data of RO signal.

## 2 Retrieving vertical Gradient of refractivity from Amplitude Data

Scheme of radio occultation experiments is shown in Fig.1. The terrestrial atmosphere is modeled locally as spherically symmetric, with a local center of curvature O. Record of radio occultation (RO) signal  $E(t)$  along the LEO trajectory is the radio hologram's envelope that contains the amplitude  $A(t)$  and phase  $\psi(t)=kS_c(t)$  of the radio field as functions of time:

$$E(t)=A(t)\exp[-i\psi(t)] \quad (1)$$

A reference signal is used to obtain high-spatial resolution and accurate estimation of refractivity from RO signals at two frequencies. Reference signal  $E_m(t)=A_m^{-1}(t)\exp[i\psi_m(t)]$  must be developed to be in maximum coherence with RO signal. This means that the phase  $\psi_m(t)$  and amplitude  $A_m(t)$  of reference signal must be connected with phase  $\psi_c(t)$  and amplitude  $A_c(t)$  of the main (coherent) part of RO signal. For achieving this aim a model of refractivity in the atmosphere and ionosphere may be applied. It is important that model must be close to real physical conditions in the radio occultation region. The functions  $A_m(t)$ ,  $\psi_m(t)$  de-

termine parameters of focused synthetic aperture and magnitude of spatial resolution.

Sliding aperture method described by *Gorbunov, 2001, section 1.3*, is equivalent to Doppler selection. In this case spatial resolution is of about 0.5-1 km and is limited by uncertainty relation (*Gorbunov, et al., 2000*). *Igarashi et al., 2000, 2001* used exponential model of the refractivity in the atmosphere and IRI-95 model for two parts of the ionosphere in the RO region to calculate temporal dependence of  $\psi_m(t)$  and obtained spatial resolution of about 20-70 m. They applied Fourier transform to product of RO and reference signal to obtain the angular spectrum  $A(\beta(\omega), p(\omega))$  of RO signal:

$$A(\beta(\omega), p(\omega)) = \int_{-T/2}^{T/2} dt E(t) E_m(t) \exp(-i\omega t); \sin\beta = \omega/(kv) + \sin\beta_m; p = \omega R_1/(kv) + p_m; \quad (2)$$

where  $\beta$  is the angle between directions PO and PG at the point P (Fig. 1),  $\beta_m, p_m$  are the angle  $\beta$  and the impact parameters  $p$  corresponding to trajectory of reference signal at the point P (Fig. 1),  $T$  is the time of coherent data handling,  $k=2\pi/\lambda; \lambda$  is the wavelength,  $v=R_1 d\theta/dt$ . Equations (2) give presentation of radio field in ray coordinates  $\beta, p$ . The second and third equations (2) allow independent measuring the functions  $p$  and  $\xi(p)$  corresponding to the main ray of RO signal and to each ray in the angular spectrum  $A(\beta, p)$  (*Hocke et al., 1999, Igarashi et al., 2000, Pavelyev et al., 2002*). Vertical resolution of the focused synthetic aperture method  $\Delta h \approx \lambda R_1/(2vT)$  (typically  $T \sim 2-3$  sec) is essentially higher than vertical resolution corresponding to the sliding aperture method. Note that canonical transform introduced by *Gorbunov, 2001*, as indicated his analysis, gives also a possibility of measurements of the refraction angle in multibeam areas at a high resolution. Usually in the lower ionosphere the electron density is not high and the single ray propagation prevails. In the case of single ray propagation, the amplitude and phase of RO signal may be considered as two independent information channels of radioholograms at frequencies  $F1$  and  $F2$ . The phase channel is usually used for estimation of the vertical profiles of the refractivity on Doppler frequency displacement (e.g. *Gorbunov et al., 1996, Feng and German, 1999, Liou and Huang, 2000*). *Pavelyev et al., (1986)* found exact solution of inverse problem for amplitude part of RO signal. Simplified form of this solution is described by:

$$p(t) - p(t_0) = \int_{t_0}^t dt X[t(p_s)] dp_s/dt; \quad p_m(t) - p_m(t_0) = \int_{t_0}^t dt X_m[t(p_s)] dp_s/dt, \quad (3)$$

where  $X_m, X$  are the power attenuation relative to free space owing to refraction effect for model and experimental data. Equation (3) allows finding the temporal dependence of impact parameter  $p(t)$  from amplitude data if initial condition is given. The power attenuation  $X(t)$  depends on the derivative  $d\xi/dp$ :

$$d\xi/dp = [1 - 1/X(t)] B(p_s); \quad B(p) = (R_1^2 - p^2)^{-1/2} + (R_2^2 - p^2)^{-1/2}. \quad (4)$$

Thus the amplitude data can be used for restoration of the functions  $p(t)$ ,  $d\xi/dp(t)$ , and the refractivity gradient  $N'_h(h)$

$$J(p) = \frac{1}{\pi} \int_p^{\infty} \frac{d\xi'_x(x)}{dx(x^2 - p^2)^{1/2}} dx; \quad N'_h(h) = -n^2(h)J(p) / \{p[1 + J(p)]\}. \quad (5)$$

The amplitude information may be used for retrieving the vertical gradient of the temperature. As shown by *Pavelyev et al., 2001*, for the case of wet atmosphere a connection exists between the vertical temperature and refractivity gradients:

$$[dT_w(h)/dh]/T_w(h) = -[N(h)]^{-1} dN(h)/dh - T_x/T_a(h), \quad (6)$$

where  $T(h)$  is the temperature of the atmosphere expressed in Kelvin's degrees. At the height above 10 km (6) may be used for finding vertical gradient of temperature if the refractivity gradient is known. It may be noted that the way of restoration of the vertical temperature and electron density profiles from amplitude data, which in some details is similar to our approach, has been considered also by *Vo-rob'ev et al., 1999*, and *Sokolovskiy, 2000*. In distinction we use model for control of multibeam and diffraction effects and apply directly our exact solution of inverse problem.

### 3 Vertical Gradients in the Mesosphere and Atmosphere

Derived in section 2 approach has been used for analysis of amplitude RO data. Experimental data are shown by the curves A1, A2 in Fig. 2 (left panel) for GPS/MET occultation event 0393, February 14, 1997. Amplitudes corresponding to reference signal at two frequencies F1, F2 are described by smooth curves M1 and M2 in Fig. 2. Amplitudes M1, M2 has been found by numerical ray tracing from model of electron density  $N_m(h)$  and its gradient  $dN_m(h)/dh$  shown in Fig. 2 (right panel) by curves 2 and 4. Curves A2, M2 are displaced for comparison. There is satisfactory correspondence between amplitudes of reference signal and experimental data. Features at levels 92 and 105 km corresponding to sporadic E-layers are clearly seen in the experimental and computed data. Retrieved by method described in section 2 vertical gradient  $dN_e(h)/dh$  (curve 5), electron density  $N_e(h)$  (curve 1) and difference  $dN_e(h)/dh - dN_m(h)/dh$  (curve 3) are shown in Fig. 2 (right panel). The highest positive maximums of  $dN_e(h)/dh$   $48 \cdot 10^9$  and  $43 \cdot 10^9$  [ $m^{-3} km^{-1}$ ] are seen at heights 92 and 105 km. Corresponding two maximums in the electron density are of about  $25 \cdot 10^9$  [ $1/m^3$ ] at levels 94 and 106 km. Also secondary maximums are seen in the Fig. 2 (right panel). Results shown in Fig. 2 illustrate sensitivity of amplitude channels of RO signal to variations of the vertical gradients of the electron density in sporadic E-layer of the ionosphere. Another example of amplitude variations that corresponds to GPS/MET occultation event June 19, 1995, No. 0583 is shown in Fig. 3 (curves A1, A2, left panel).

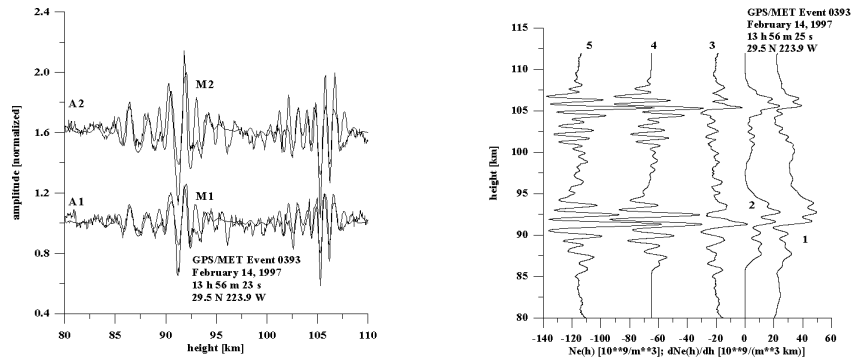


**Fig. 2.** Left panel. Comparison of amplitude variations A1, A2 at two frequencies with amplitudes of reference signal (smooth curves M2, M1). Right panel. Results of restoration of vertical distribution of the electron density  $N_e(h)$  and its gradient  $dN_e(h)/dh$ . Curves 1, 3, 4, 5 are displaced by  $20 [10^9/m^3]$ ;  $-20$ ;  $-65$ ;  $-115 [10^9/m^3 km^{-1}]$ , respectively.

Smooth curves M in Fig. 3 show amplitude of reference signals calculated by ray tracing from models of  $N_m(h)$ ,  $dN_m(h)/dh$  (curves 2, 4, right panel). Amplitude variations A1, A2 are strongly correlated, their level is proportional to the ratio  $f_2^2/f_1^2$  demonstrating their ionospheric origin. In the amplitude data influence of sporadic E-layer structure can be seen at the heights 90-94 km and 98-100 km. Retrieved vertical profiles  $N_e(H)$  and its gradient  $dN_e(H)/dH$  are shown in Fig. 3, right panel, by curves 1, 4, respectively. The maximum value of the negative gradient of about  $-46 \cdot 10^9 [m^{-3} km^{-1}]$  is located at height 94.5 km (curve 4 in Fig. 3). The vertical profile  $N_e(h)$  (curve 1 in Fig. 3) coincides with its gradient  $dN_e(h)/dh$  (curve 4) showing feature at 94 km with maximum of about  $50 \cdot 10^9 [m^{-3}]$ .

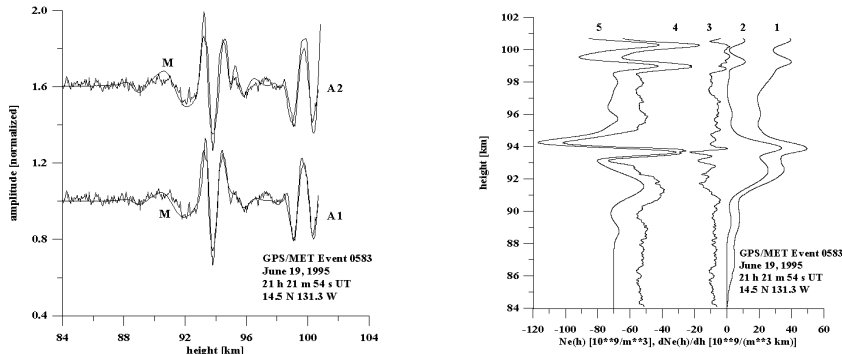


**Fig. 3.** Left panel. Comparison of amplitude variations A1, A2 at two frequencies with amplitudes of reference signal M (smooth curves M). Right panel. Results of restoration of vertical distribution of the electron density  $N_{em}(h)$  and its gradient  $dN_e(h)/dh$ . Curves 3, 4, 5 are displaced by  $-10$ ;  $-55$ ;  $-70 [10^9/m^3 km^{-1}]$  respectively. Curve 3 represents difference  $dN_e/dh - dN_m/dh$ .

Analysis of information containing in the amplitude channels of RO signal gives detailed picture of vertical gradient distribution in the lower ionosphere. This is important because Earth-based tools usually give vertical profiles of the electron density distribution below their maximum. Vertical gradients of refractivity may be studied in the atmosphere also using amplitude channels of RO signal. For example amplitude variations at frequency F1 are shown in Fig. 4 (curve A) for CHAMP RO event 09 (April 06, 2001). Normalized amplitude variations shown in Fig. 4 are scaled by 20 and displaced by 10 for comparison with retrieved vertical gradient of the temperature  $dT/dh$  (curve B) and refractivity  $dN/dh$  (curves C, D). Smooth curve A in Fig. 4 corresponds to amplitude changes owing to standard vertical distribution of the refractivity  $N(h)=332\exp(-h/8)$  [N-unit]. Curve A accounts for the absorption in oxygen at small height also. As seen from Fig. 4 the regular refraction attenuation (with absorption) changes from 0.3 (at height 3 km) up to 1 (at height 40 km). Curve A, in average, gives good approximation to experimental amplitude variations. Measured amplitude variations are intense in the height interval 3-18 km. Quasi-periodical structures are seen in amplitude variations between levels 10 and 25 km. Above 25 km the amplitude variations are smaller. Curve D in Fig. 4 shows variations in the vertical gradients in the height interval 3-37 km. Curve C is scaled version of the curve D. Curve C shows small changes of the vertical gradient of refractivity at the heights 12 to 37 km. At the

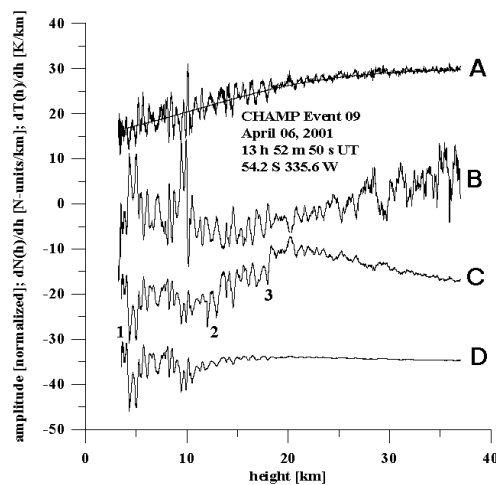


**Fig. 4.** Comparing amplitude variations at the first CHAMP frequency (curve A), retrieved vertical gradient of refractivity  $dN(h)/dh -G_s(h)-20$ ;  $dN(h)/dh -G_s(h)-35$  [N-units/km] (curves C, D) and temperature  $dT(h)/dh$  (curve B). Curve C is scaled by 5 times in interval 2-3 (heights between 12 and 18 km), and by 10 times at heights above 18 km. Scaling is absent in the interval 1-2 (heights between 3 and 12 km). Vertical gradient  $G_s(h)$  corresponds to model A used for calculation of refraction attenuation:  $G_s(h)=-42 \exp(-h/8)$  [N-units/km].

height levels between 3-11 km variations of the vertical gradient of refractivity are about of  $\pm 5$  N-units/km. In the tropopause area (heights between 12-19 km) the variations of vertical gradient  $dN/dh$  are about  $\pm 2$  N-units/km. Vertical distribution of temperature gradient between level 3-37 km (curve B) reveals features at height 4-6, 9-10 km with positive values of about 6-9 °K/km. Vertical distribution of temperature gradient reveals waves structures with spatial period 0.8-4 km. These variations may be connected with propagation of internal waves in the atmosphere.

## 4 Conclusion

It is shown that amplitude channel of RO signals may be used independently from phase channel for detailed retrieving the vertical profiles of the refractivity gradient in the atmosphere and ionosphere. Amplitude channel is less sensitive to upper ionosphere contribution than phase channel. The first results of measurements of refractivity gradients in the equatorial atmosphere revealed layered structure below tropopause in the troposphere. Fine structures in the vertical gradient of electron density have been retrieved from RO amplitude channels in the sporadic E-layers (heights interval 92-105 km). This demonstrates that amplitude method may be used for high-precision measurements of atmospheric and ionospheric parameters in existing CHAMP and future COSMIC RO mission.

**Acknowledgements.** We are grateful to UCAR for access to the GPS/MET data. We are grateful to National Science Council of Taiwan, R.O.C., for financial support under the grants NSC 91-2811-M008-001, NSC 90-2111-M008-047-AGC, and Office of Naval Research (ONR) of USA under grant N00014-00-0528. Work has been partly supported by Russian Fund of Basic Research, grant No. 01-02-17649.

## References

- Feng DD and Herman BM (1999) Remotely sensing the Earth's atmosphere using the Global Positioning System (GPS) - the GPS/MET data analysis. *Journal of Atmospheric and Ocean Technology* **16**, 990-1002.
- Gorbunov ME, Gurvich AS, Bengtsson L (1996) Advanced algorithms of inversion of GPS=MET satellite data and their application to reconstruction of temperature and humidity. Report 211, Max-Planck-Institute for Meteorology ISSN0937-1060.
- Gorbunov ME (2001) Radio holographic methods for processing radio occultation data in multipath regions. *Scientific report 01-02*. Danish Meteorological Institute (DMI), Copenhagen.
- Gorbunov ME, Gurvich AS, and Shmakov AV (2002) Back-propagation and radio-holographic methods for investigation of sporadic ionospheric E-layers from Microlab-1 data. *Int J Remote Sensing*, **23**, No 4, 675-685.

- Gorbunov ME, Gurvich AS, and Kornblueh L (2000) Comparative analysis of radio-holographic methods of processing radio occultation data, *Radio science*, **35**, No 4, 1025-1034.
- Hocke K, Pavelyev A, Yakovlev O, Barthes L and Jakowski N (1999) Radio occultation data analysis by radio holographic method. *JASTP*, **61**, P 1169-1177.
- Igarashi K, Pavelyev A, Hocke K, Pavelyev D, and Wickert J (2001) Observation of wave structures in the upper atmosphere by means of radio holographic analysis of the radio occultation data. *Advances in Space Research*, **27**, No 6-7, 1321-1327.
- Igarashi K, Pavelyev A, Wickert J, Hocke K, Pavelyev D (2002) Application of radio holographic method for observation of altitude variations of the electron density in the mesosphere/lower thermosphere using GPS/MET radio occultation data. *JASTP*, **64**, in press.
- Igarashi K, Pavelyev A, Hocke K, Pavelyev D, Kucherjavenkov I, Matugov S, Zakharov A, and Yakovlev O (2000) Radio holographic principle for observing natural processes in the atmosphere and retrieving meteorological parameters from radio occultation data. *Earth Planets Space*, **52**, 968-875.
- Karayel ET, and Hinson DP (1997) Sub-Fresnel-scale vertical resolution in atmospheric profiles from radio occultation. *Radio science*, **32**, No 2, 411-428.
- Marouf EA, and Tyler GL (1982) Microwave edge diffraction by features in Saturn's rings: Observations with Voyager 1. *Science* **217**, 243-245.
- Lindal GF., Lyons JR, Sweetnam DN, Eshleman VR, Hinson DP, and Tyler GL (1987) The atmosphere of Uranus: Results of radio occultation measurements with Voyager 2, *J Geophys Res*, **92** (A13), 14,987--15,001.
- Pavelyev A, Yakovlev OI, Matyugov SS, Pavelyev D, Anufriev VA (2001) Advanced algorithms of inversion of GPS radio limb sounding data. Scientific Technical Report STR01/06. GeoForschungZentrum Potsdam. *and Electronics*, **43**, No. 8, 126-131, 1998.
- Pavelyev A, Matyugov S, Kalashnikov I, and Yakovlev O (1986) Analysis of the features of radio occultation method for the Earth's atmosphere study. In the book *Electromagnetic waves in the atmosphere and space*, pp 208-218. "Nauka" Ed Moscow, 1986 (in Russian).
- Pavelyev A, Igarashi K, Reigber Ch, Hocke K, Wickert J, Beyerle G, Matugov S, Kucherjavenkov S, Pavelyev D, and Yakovlev OI (2002) First application of the radio holographic method to wave observation in the upper atmosphere. *Radio science*, **37**, in press.
- Sokolovskiy SV (2000) Inversion of radio occultation amplitude data, *Radio Science*, **35**(1), 97-105.
- Sokolovskiy SV, Schreiner W, Rocken C, Hunt D (2002) Detection of high-altitude ionospheric irregularities with GPS/MET, *Geophys Res Letters*, **29**(3), 621-625.
- Vorob'ev VV, Gurvich AS, Kan V, Sokolovskiy SV, Fedorova OV, Shmakov AV (1999) Structure of the ionosphere from the radio-occultation GPS-"Microlab-1" satellite data: preliminary results. *Earth Observations and Remote Sensing* **15**, 609-622.
- Yuei-An Liou, and Cheng-Yung Huang (2000) Active Limb Sounding of Atmospheric Refractivity, Pressure, and Temperature Profiles from GPS Occultation by 3-D Vector Analysis. *Proceedings of COSMIC International Workshop. September 27-29, 2000*, pp 60-69. Taipei, Taiwan.